Supporting Information

Complementary GIXRD Analysis

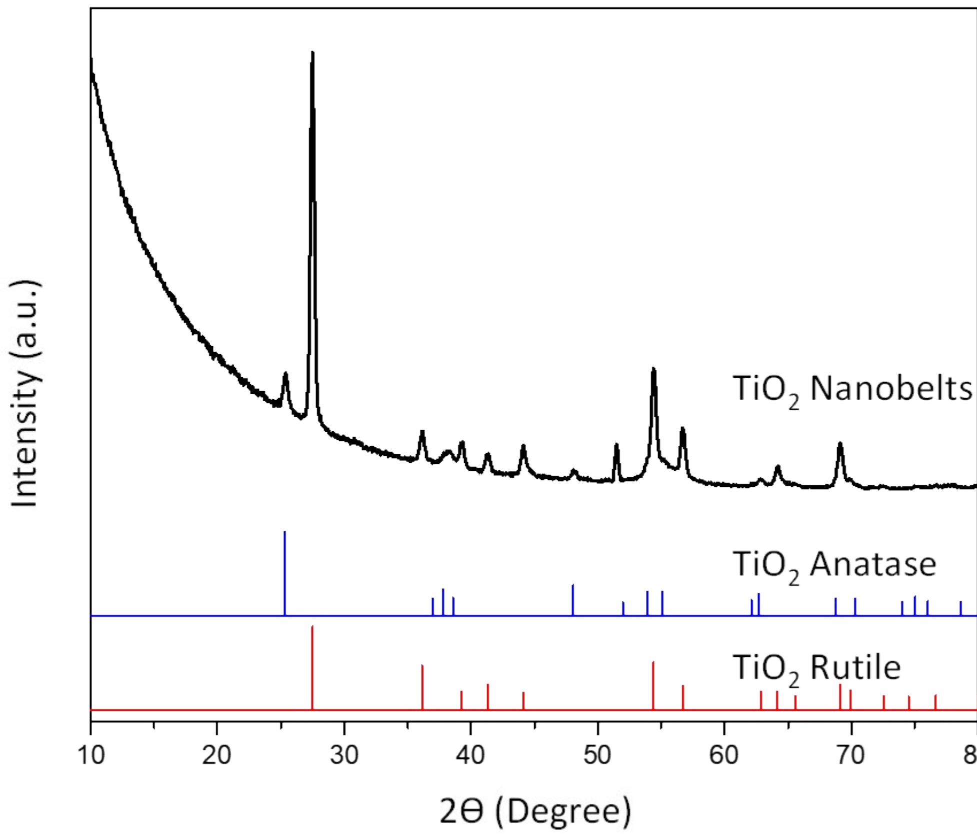

Figure S1. The GIXRD pattern of TiO_2 nanobelts grown by catalyst-assisted PLD.

Table S1. Comparison of the position shifts of the two prominent (111) and (200) peaks in $Hf_{1-x}Ti_xO_2$ nanospikes relative to their respective peaks in the undoped HfO_2 NWs.

Plane Index	HfO_2 Nanowires 2θ (°)	$Hf_{0.99}Ti_{0.01}O_2$ Nanopikes		$Hf_{0.90}Ti_{0.10}O_2$ Nanopikes		$Hf_{0.75}Ti_{0.25}O_2$ Nanopikes	
		2θ (°)	Shift (°)	2θ (°)	Shift (°)	2θ (°)	Shift (°)
(1 1 1)	31.71	31.73	0.02	31.80	0.09	31.75	0.04
(2 0 0)	34.37	34.38	0.01	34.44	0.07	34.44	0.07

EDS Elemental Analysis of $Hf_{1-x}Ti_xO_2$ Nanospikes

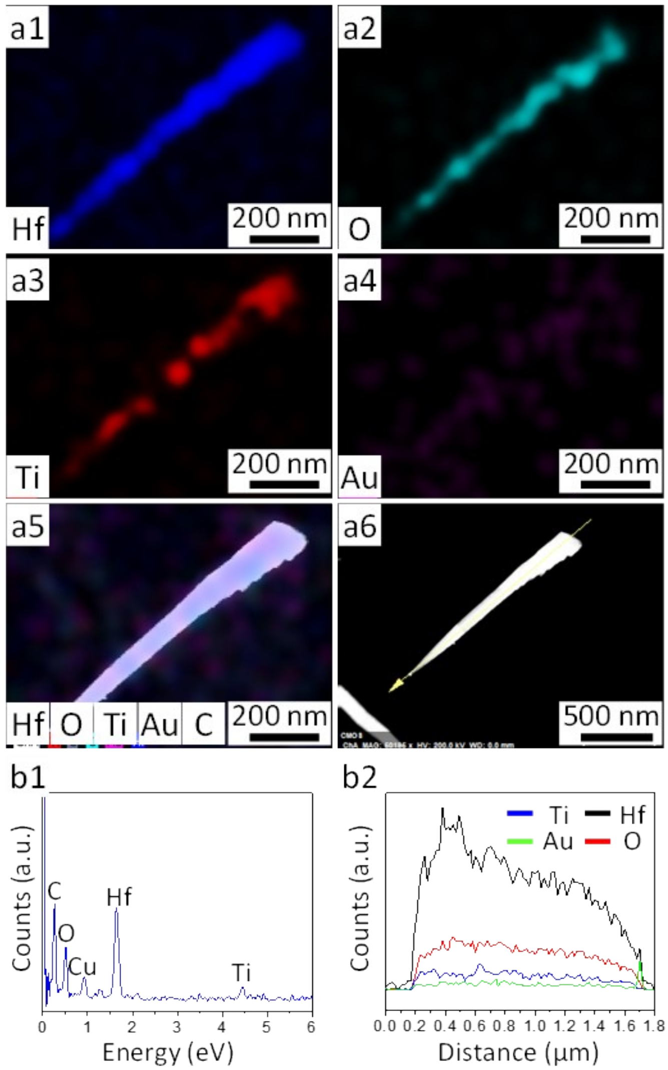

Figure S2. (a) STEM-EDS elemental maps for (a1) Hf, (a2) O, (a3) Ti, (a4) Au, and (a5) their overlaps of a $Hf_{0.75}Ti_{0.25}O_2$ nanospike grown on a Sn-GNI/Ox-Si substrate at 770 °C, along with (a6) its STEM High-Angle Annular Dark Field (STEM-HAADF) image. The corresponding (b1) EDS spectrum of the elemental maps, and (b2) the EDS linescan profiles of Hf, O, Ti and Au along the nanospike marked in (a6).

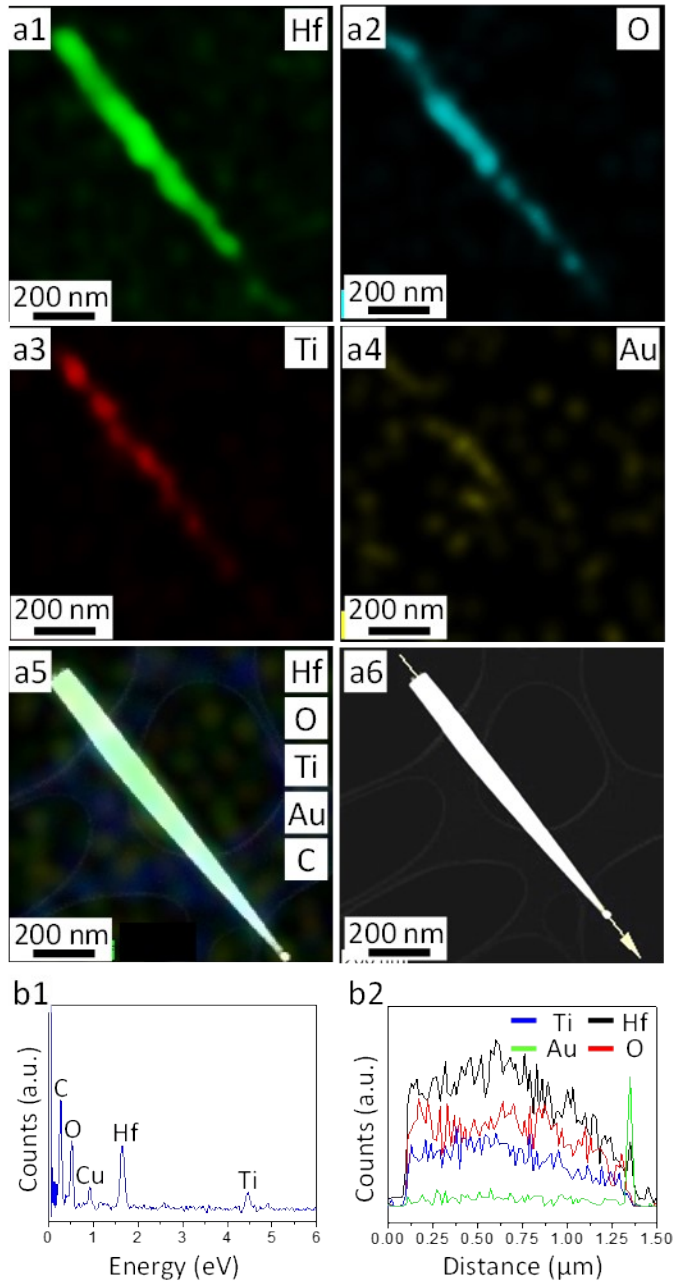

Figure S3. (a) STEM-EDS elemental maps for (a1) Hf, (a2) O, (a3) Ti, (a4) Au, and (a5) their overlaps of a $Hf_{0.50}Ti_{0.50}O_2$ nanospike grown on a Sn-GNI/Ox-Si substrate at 770 °C, along with (a6) its STEM High-Angle Annular Dark Field (STEM-HAADF) image. The corresponding (b1) EDS spectrum of the elemental maps, and (b2) the EDS linescan profiles of Hf, O, Ti and Au along the nanospike marked in (a6).

Comparison of Magnetic Properties of $Hf_{1-x}Ti_xO_2$ Nanostructures with Previous Studies on HfO_2 and ZrO_2

Table S2. Comparison of magnetic properties of $Hf_{1-x}Ti_xO_2$ ($0 \leq x \leq 1$) nanostructures with those of ZrO_2 and HfO_2 in previous studies.

Sample	Measurement Temperature (K)	M_s (emu/g)	M_r (emu/g)	H_c (Oe)
HfO_2 nanowires[a]	300	1.2×10^{-3}	0.8×10^{-4}	29
	2	2.5×10^{-3}	2.0×10^{-4}	160
$Hf_{0.99}Ti_{0.01}O_2$ nanospikes[a]	300	1.4×10^{-3}	3.2×10^{-4}	312
	2	4.2×10^{-3}	7.3×10^{-4}	362
$Hf_{0.90}Ti_{0.10}O_2$ nanospikes[a]	300	2.3×10^{-3}	3.2×10^{-4}	431
	2	4.8×10^{-3}	7×10^{-4}	547
TiO_2 Nanobelts[a]	300	3.9×10^{-3}	1.7×10^{-3}	702
	2	21.1×10^{-3}	2.5×10^{-3}	597
HfO_2 thin film[1]	300	1-100.1	-	-
HfO_2 thin film[2]	300	3	-	-
HfO_2 thin film[3]	300	2	-	115
	1.8	5	-	-
HfO_2 colloidal nanorods[4]	300	1.3×10^{-2}	-	300
	10	2.3×10^{-2}	-	50
ZrO_2 nanowires[5]	300	5.9	1.5	99
	5	8.5	2	100
ZrO_2 nanoclusters[6]	300	1.8	0.12	77
	5	1.9	0.2	120

[a]This work.

Surface Analysis

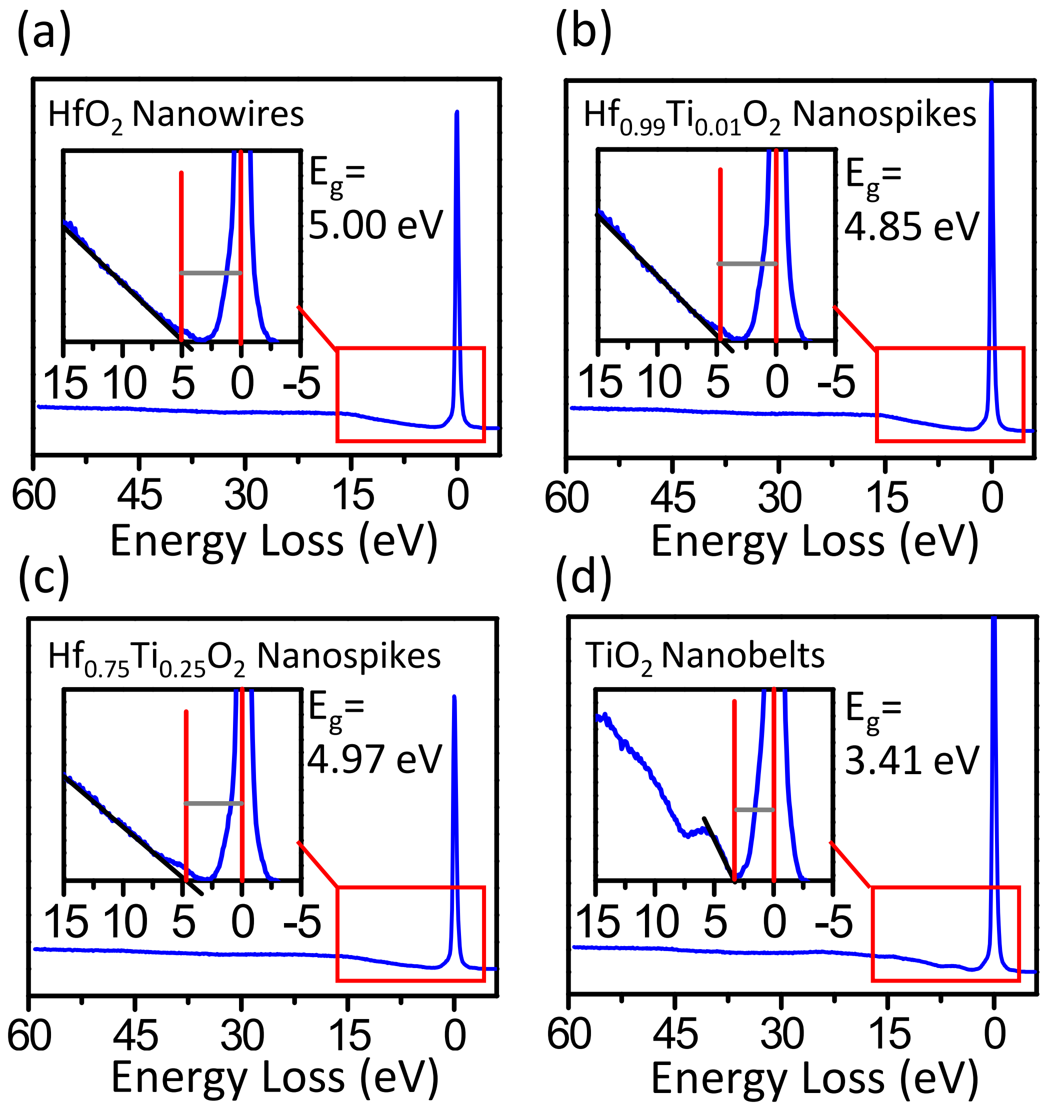

Figure S4. Electron energy loss spectra of (a) HfO_2 nanowires, (b) $Hf_{0.99}Ti_{0.01}O_2$ nanospikes, (c) $Hf_{0.75}Ti_{0.25}O_2$ nanospikes and (d) TiO_2 nanobelts. Insets show the determination of the bandgap by using linear fittings on the onsets of loss signal spectra.

Additional Magnetization Measurements

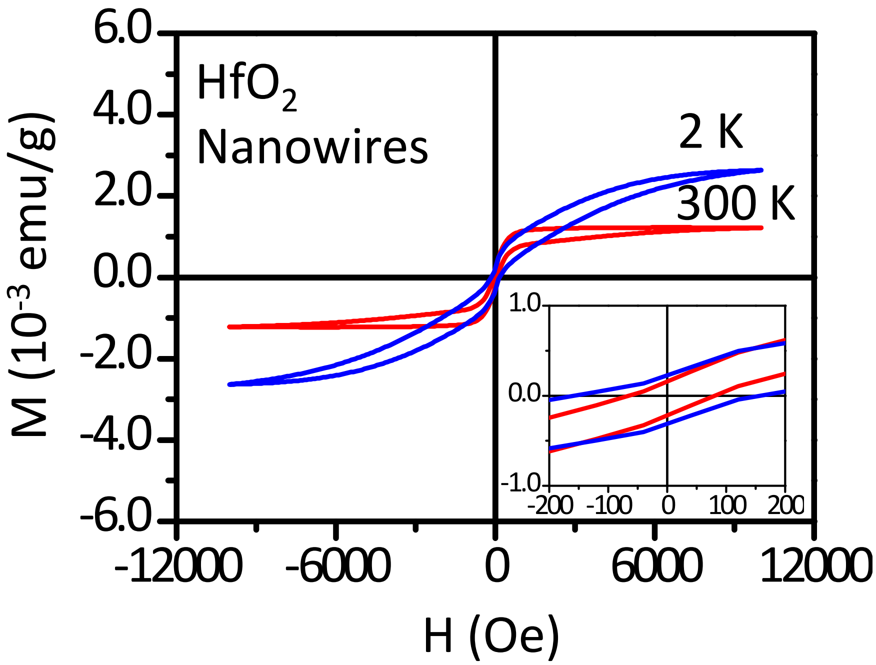

Figure S5. Magnetization (M) as a function of applied magnetic field (H) of undoped HfO_2 nanowires.[7]

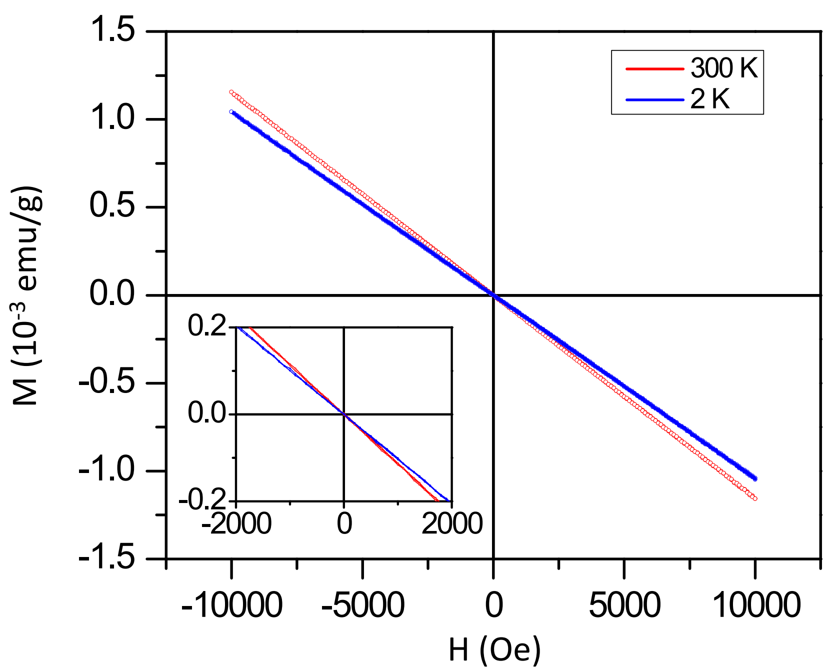

Figure S6. Magnetization (M) as a function of the applied magnetic field (H) of bare Si substrate, measured at 2 K and 300 K.

Surface Analysis and Depth-profiling

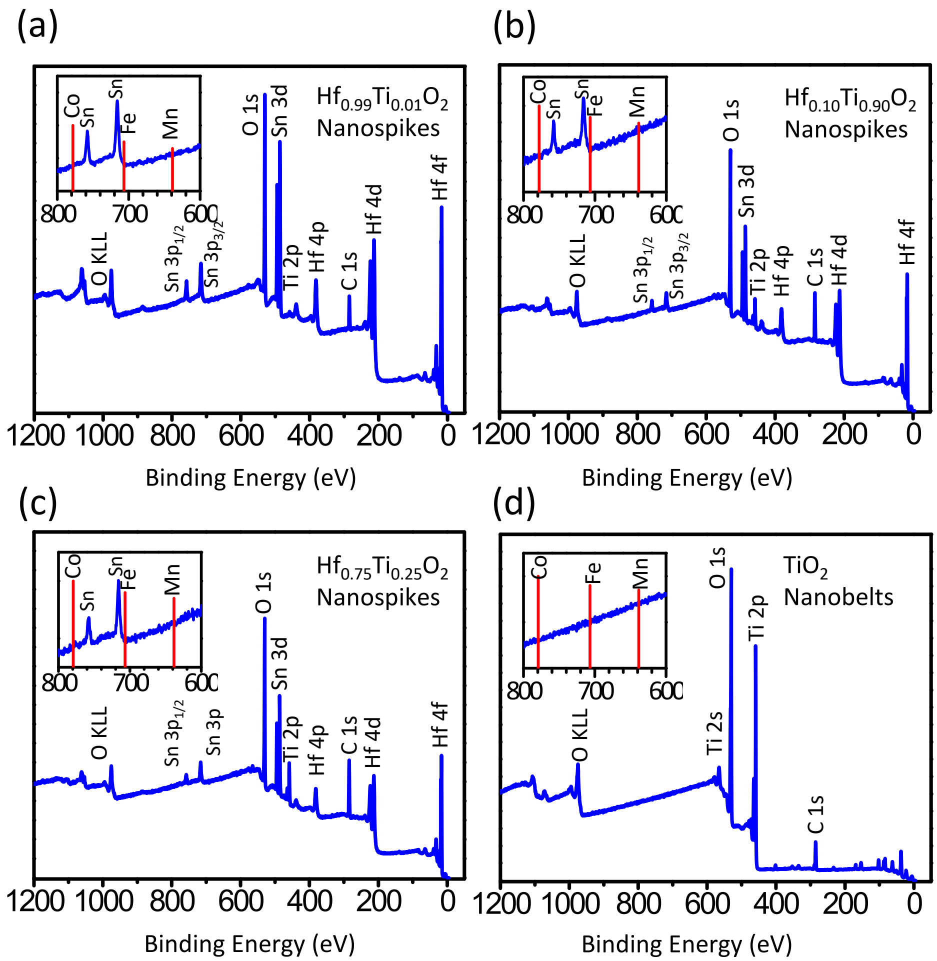

Figure S7. XPS survey spectra of (a) $Hf_{0.99}Ti_{0.01}O_2$ nanospikes (b) $Hf_{0.90}Ti_{0.10}O_2$ nanospikes (c) $Hf_{0.75}Ti_{0.25}O_2$ nanospikes, and (d) TiO_2 nanobelts. The insets show expanded views of the Mn, Fe and Co spectral regions.

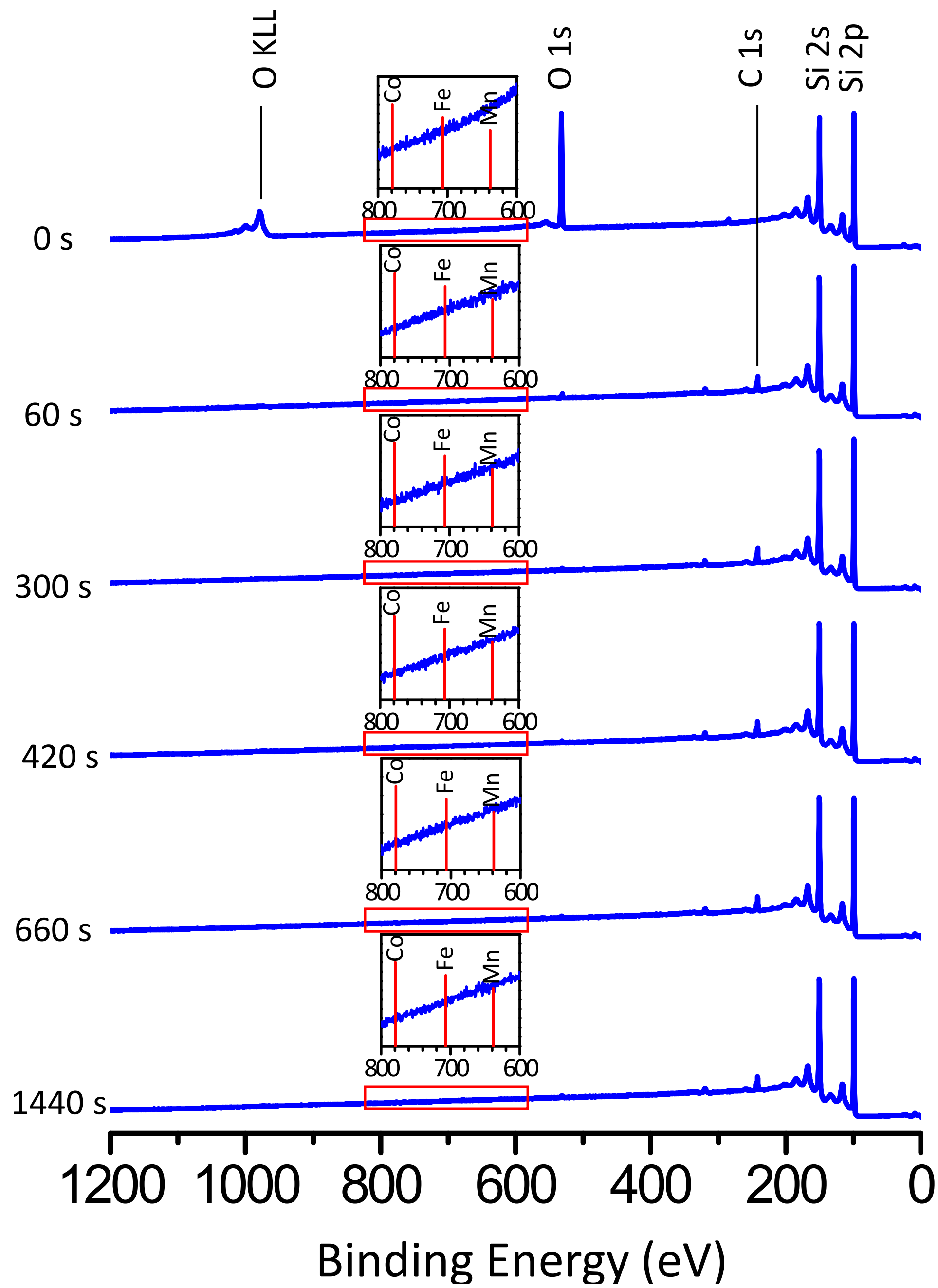

Figure S8. XPS depth-profiling survey spectra of the Si substrate with increasing Ar sputtering time. Insets show expanded views of the Mn, Fe, and Co spectral regions.

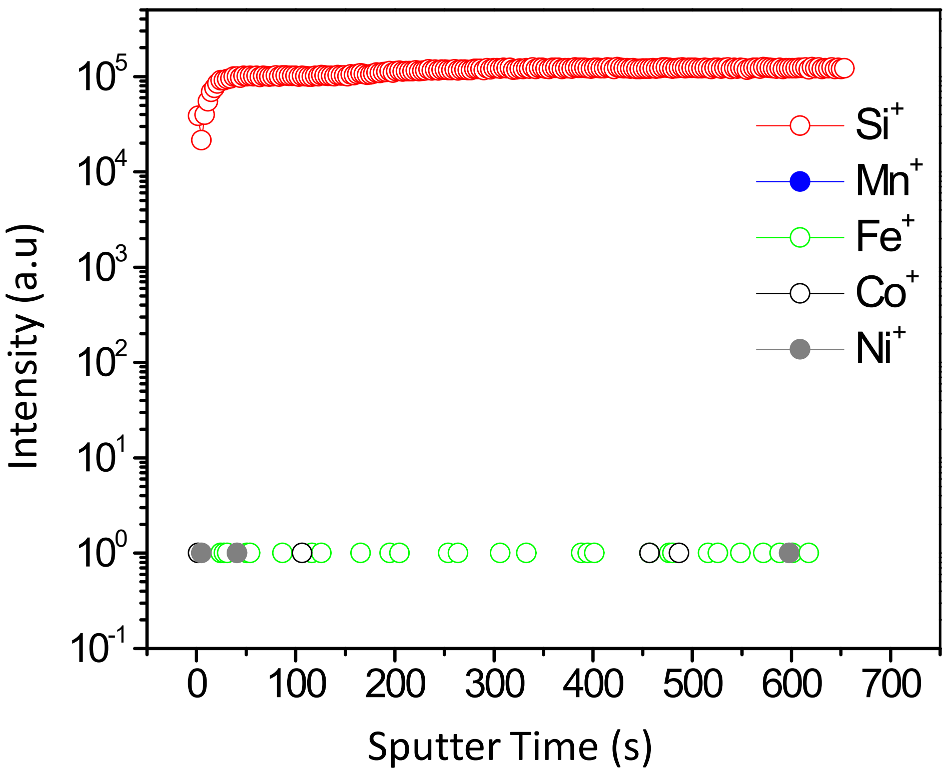

Figure S9. TOF-SIMS depth profile of the Si substrate during 700 s of Ar sputtering. With the exception of Si^+, all the other ion signals are found to overlap with one another.

References

1 J. M. D. Coey, M. Venkatesan, P. Stamenov, C. B. Fitzgerald and L. S. Dorneles, *Phys. Rev. B - Condens. Matter Mater. Phys.*, 2005, **72**, 024450.

2 N. H. Hong, J. Sakai, N. Poirot and V. Brizé, *Phys. Rev. B - Condens. Matter Mater. Phys.*, 2006, **73**, 132404.

3 K. K. Bharathi, S. Venkatesh, G. Prathiba, N. H. Kumar and C. V. Ramana, *J. Appl. Phys.*, 2011, **109**, 07C318.

4 E. Tirosh and G. Markovich, *Adv. Mater.*, 2007, **19**, 2608–2612.

5 M. A. Rahman, S. Rout, J. P. Thomas, D. McGillivray and K. T. Leung, *J. Am. Chem. Soc.*, 2016, **138**, 11896–11906.

6 X. Guan, S. Srivastava, J. P. Thomas, N. F. Heinig, J. S. Kang, M. A. Rahman and K. T. Leung, *ACS Appl. Mater. Interfaces*, 2020, **12**, 48998–49005.

7 M. Beedel, M. A. Rahman, H. Farkhondeh, J. P. Thomas, L. Zhang, N. F. Heinig and K. T. Leung, *Mater. Today Nano*, 2024, **28**, 100510.